Electronic Supplementary Material (ESI) for Journal of Materials Chemistry C.

Supporting Information

Highly Flexible Cellulose Nanofiber/Single-crystal Nanodiamond Flake Heat Spreader Films for Heat Dissipation

Ping Gong[1, 2#], Linhong Li[1, 2#], Guang-en Fu[1, 2], Shengcheng Shu[1], Maohua Li[1], Yandong Wang[1], Yue Qin[1], Xiangdong Kong[1], Huanyi Chen[1], Chengcheng Jiao[1], Xinxin Ruan[1], Tao Cai[1,2], Wen Dai[1], Chao Yan[3], Kazuhito Nishimura[4], Cheng-Te Lin [1, 2], Nan Jiang* [1, 2], Jinhong Yu*[1,2]*

[1]*Ningbo Institute of Materials Technology and Engineering, Chinese Academy of Sciences, Ningbo,315201, China.*

[2]*Center of Materials Science and Optoelectronics Engineering, University of Chinese Academy of Sciences, Beijing 100049, China.*

[3]*School of Materials Science and Engineering, Jiangsu University of Science and Technology, Zhenjiang, 212003, PR China*

[4]*Advanced Nano-processing Engineering Lab, Mechanical Engineering, Kogakuin University, Tokyo, 192-0015, Japan.*

Corresponding author, E-mail:** ***chaoyan@just.edu.cn (C. Yan); jiangnan@nimte.ac.cn (N. Jiang); yujinhong@nimte.ac.cn (J. Yu).

[#]*Both authors are co-first authors and contributed equally to this work.*

Supplementary Materials

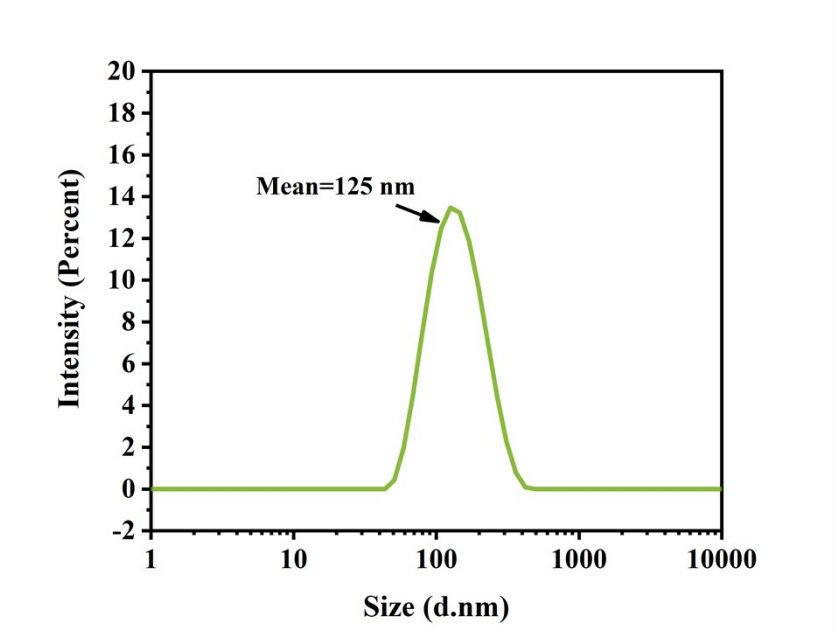

Figure S1. The size distribution of SCND.

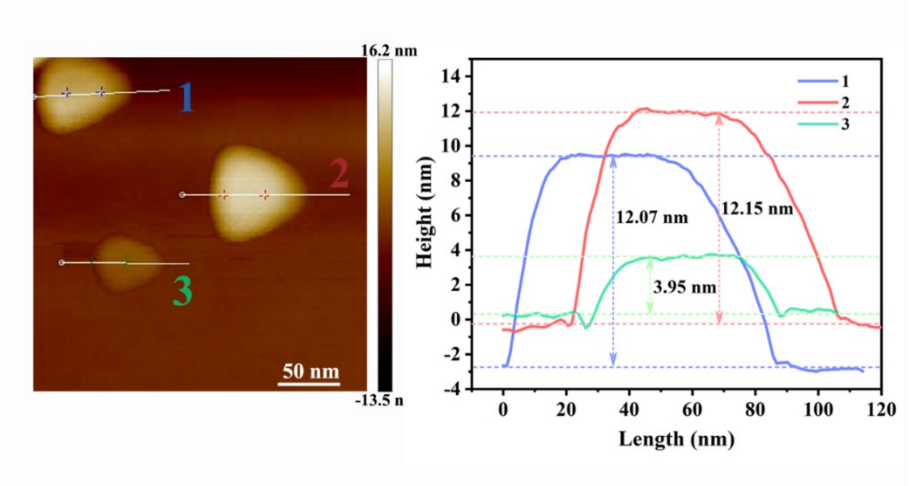

Figure S2. (**a**) AFM image of SCND; (**b**) The corresponding height profile.

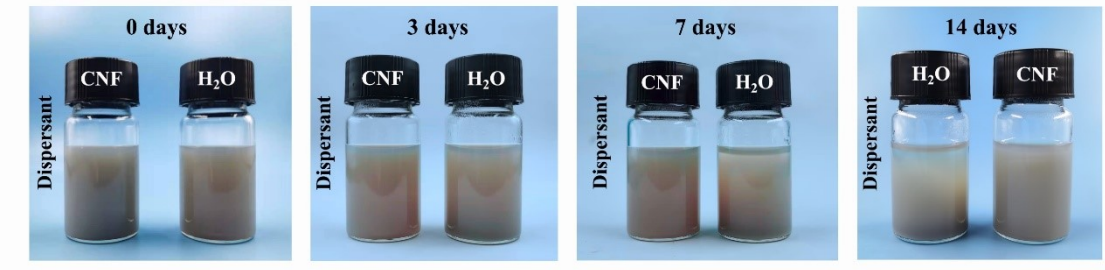

Figure S3. Photographs of SCND dispersion in H_2O and CNF aqueous solution from 0 to 14 days.

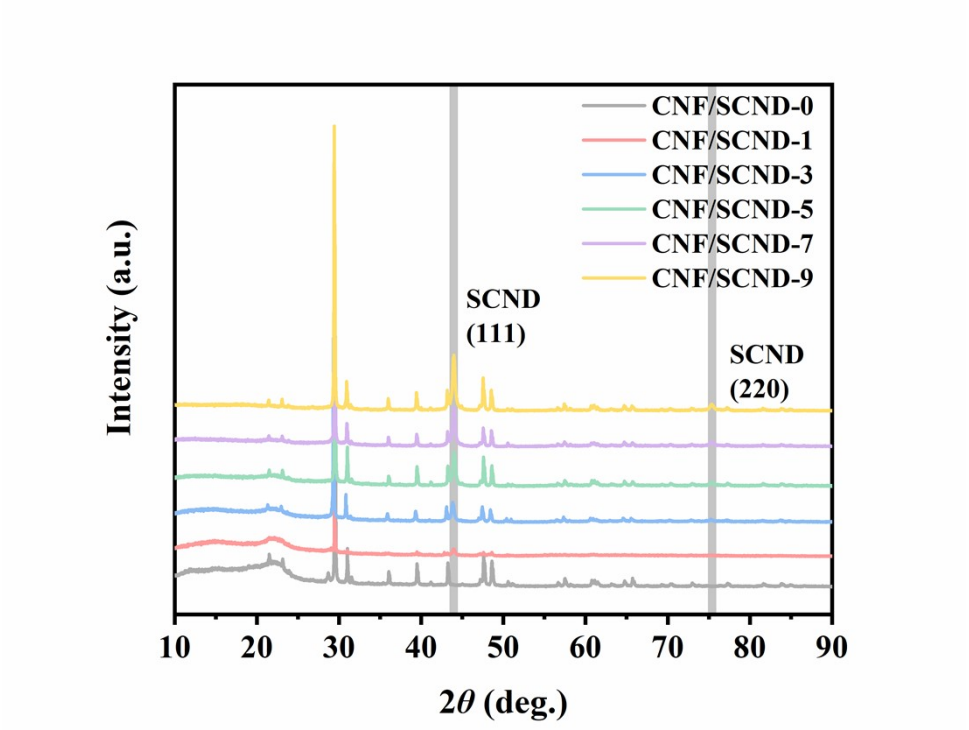

Figure S4. XRD patterns of the CNF/SCND composite films.

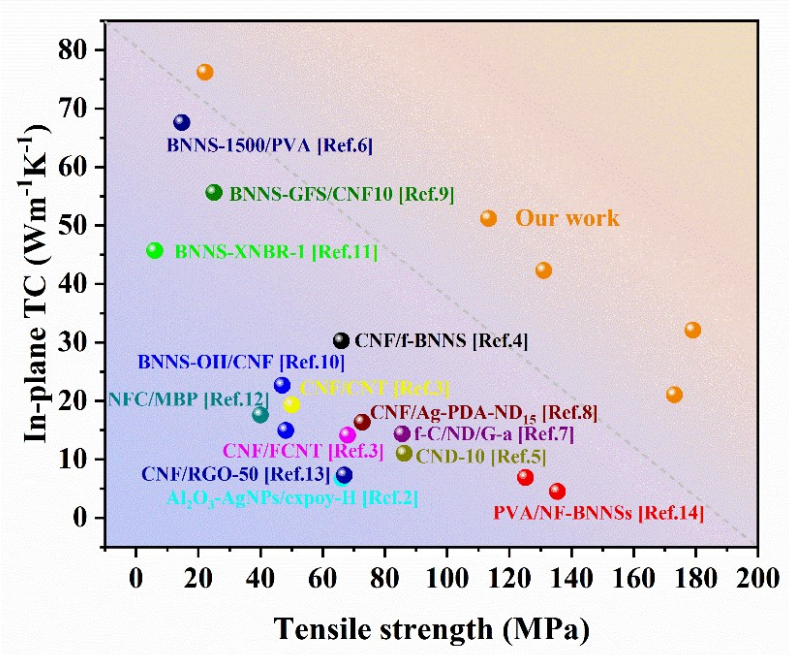

Figure S5: Comparison of the thermal conductivity and tensile strength of the CNF/SCND composite films with those of other similar references[2-14].

Table S1. The theoretical binding energies calculated by the relative content and actual test values of CNF/SCND composite films.

Sample	SCND Contents (wt%)	CNF Contents (wt%)	Theoretical binding energy (eV)	Test binding energy (eV)
CNF/SCND-0	0	100	/	529.46
CNF/SCND-1	10	90	529.63	529.54
CNF/SCND-3	30	70	529.98	529.60
CNF/SCND-5	50	50	530.33	529.65
CNF/SCND-7	70	30	530.68	529.54
CNF/SCND-9	90	10	531.03	529.63
SCND	100	/	/	531.2

Table S2. The parameters for the calculation of in-plane thermal conductivities of pure CNF and CNF/SCND composite films.

Sample	SCND Contents (wt%)	Thermal diffusivity (mm^2s^{-1})	Specific heat capacity ($J\,g^{-1}K^{-1}$)	Density ($g\,cm^{-3}$)	Thermal conductivity ($W\,m^{-1}K^{-1}$)
CNF/SCND-0	0	0.23 ± 0.01	1.499	1.616	0.52 ± 0.02
CNF/SCND-1	10	8.69 ± 0.06	1.457	1.716	21.07 ± 0.14
CNF/SCND-3	30	10.36 ± 0.44	1.385	2.05	29.34 ± 1.36
CNF/SCND-5	50	15.58 ± 0.79	1.242	2.186	42.3 ± 2.13
CNF/SCND-7	70	21.73 ± 0.41	0.991	2.378	51.22 ± 0.97
CNF/SCND-9	90	33.41 ± 1.12	0.732	3.117	76.23 ± 2.56

[1] H. Zeng, J. Wu, H. Pei, et al. Highly thermally conductive yet mechanically robust composites with nacre-mimetic structure prepared by evaporation-induced self-assembly approach [J]. Chemical Engineering Journal, 2021, 405: 126865.

[2] G. Pan, Y. Yao, X. Zeng, et al. Learning from Natural Nacre: Constructing Layered Polymer Composites with High Thermal Conductivity [J]. ACS Appl Mater Interfaces, 2017, 9(38): 33001-10.

[3] X. Wang, P. Wu. Fluorinated Carbon Nanotube/Nanofibrillated Cellulose Composite Film with Enhanced Toughness, Superior Thermal Conductivity, and Electrical Insulation [J]. ACS Appl Mater Interfaces, 2018, 10(40): 34311-21.

[4] K. Wu, J. Fang, J. Ma, et al. Achieving a Collapsible, Strong, and Highly Thermally Conductive Film Based on Oriented Functionalized Boron Nitride Nanosheets and Cellulose Nanofiber [J]. ACS Appl Mater Interfaces, 2017, 9(35): 30035-45.

[5] N. Song, S. Cui, X. Hou, et al. Significant Enhancement of Thermal Conductivity in Nanofibrillated Cellulose Films with Low Mass Fraction of Nanodiamond [J]. ACS Applied Materials & Interfaces, 2017, 9(46): 40766-73.

[6] Q. Yan, W. Dai, J. Gao, et al. Ultrahigh-Aspect-Ratio Boron Nitride Nanosheets Leading to Superhigh In-Plane Thermal Conductivity of Foldable Heat Spreader [J]. ACS Nano, 2021, 15(4): 6489-98.

[7] S. Cui, N. Song, L. Shi, et al. Enhanced Thermal Conductivity of Bioinspired Nanofibrillated Cellulose Hybrid Films Based on Graphene Sheets and Nanodiamonds [J]. ACS Sustainable Chemistry & Engineering, 2020, 8(16): 6363-70.

[8] S. Yang, X. Sun, J. Shen, et al. Interface Engineering Based on Polydopamine-Assisted Metallization in Highly Thermal Conductive Cellulose/Nanodiamonds Composite Paper [J]. ACS Sustainable Chemistry & Engineering, 2020, 8(48): 17639-50.

[9] W. Qiu, W. Lin, Y. Tuersun, et al. Ultra-Flexible, Dielectric, and Thermostable Boron Nitride-Graphene Fluoride Hybrid Films for Efficient Thermal Management [J]. Advanced Materials Interfaces, 2021, 8: 2002187.

[10]Z. Hu, S. Wang, G. Chen, et al. An aqueous-only, green route to exfoliate boron nitride for preparation of high thermal conductive boron nitride nanosheet/cellulose nanofiber flexible film [J]. Composites Science and Technology, 2018, 168: 287-95.

[11]X. Wu, W. Liu, C. Zhang, et al. Grafting rubber chains onto boron nitride nanosheets for highly

flexible, thermally conductive composites [J]. European Polymer Journal, 2018, 100: 12-7.

[12]J. Hu, H. Xia, X. Hou, et al. Enhanced thermal management performance of nanofibrillated cellulose composite with highly thermally conductive boron phosphide [J]. Journal of Materials Chemistry A, 2021, 9(47): 27049-60.

[13]W. Yang, Z. Zhao, K. Wu, et al. Ultrathin flexible reduced graphene oxide/cellulose nanofiber composite films with strongly anisotropic thermal conductivity and efficient electromagnetic interference shielding [J]. Journal of Materials Chemistry C, 2017, 5(15): 3748-56.

[14]X. Zeng, L. Ye, S. Yu, et al. Artificial nacre-like papers based on noncovalent functionalized boron nitride nanosheets with excellent mechanical and thermally conductive properties [J]. Nanoscale, 2015, 7(15): 6774-81.